Water Splitting

Molybdenum Boride and Carbide Catalyze Hydrogen Evolution in both Acidic and Basic Solutions**

Heron Vrubel and Xile Hu*

Sunlight-driven water splitting is one of the most attractive methods for solar energy conversion and storage.[1] To achieve efficient water splitting, active catalysts for the hydrogen evolution reaction (HER) are required.[2] Although platinum and a few other precious metals are highly active HER catalysts, their high cost and low abundance are severe hurdles for large-scale applications. The limitations of precious HER catalysts prompts the search for and development of non-precious catalysts.[3] Molybdenum-based materials and molecules have drawn much attention recently.[4–7] In particular, molybdenum sulfides have been shown to exhibit high HER activity.[4–6] There is experimental and computational evidence that the active sites in these catalysts are located at the Mo edge, where there are unsaturated sulfur atoms.[4] These sulfur atoms can adsorb hydrogen atoms and mediate hydrogen evolution.

Herein, we report that molybdenum boride (MoB) and carbide (Mo_2C) are active HER catalysts. To our knowledge, this is the first time MoB has been shown to be a HER catalyst. Although Mo_2C has been shown to be a good support for Pt in HER,[8] its own HER activity has not been studied in detail.[9] Our results are interesting in several aspects: 1) The catalysts are non-precious and commercially available. They are also active under both acidic and basic conditions, which are rare properties for HER catalysts. 2) As the structures of molybdenum boride and carbide are different from that of MoS_2, the activity of these catalysts is not easily explained by the presence of unsaturated edge sites. The results presented here might invoke new theoretical and experimental investigations of molybdenum-containing HER catalysts. 3) The work might inspire the development of molecular catalysts containing unusual boride and carbide ligands.[10]

MoB and Mo_2C particles were purchased from commercial sources and their compositions were confirmed by inductively coupled plasma optical emission spectrometry (ICP-OES). XRD measurements showed that the MoB

particles were mainly in the α-form (tetragonal), whereas the Mo_2C particles were in the β-form (hexagonal; Supporting Information, Figure S1). According to SEM images, the particle size is in the range of 1–3 μm (Figure S2). The MoB and Mo_2C particles were deposited onto carbon-paste electrodes so that their HER activity could be measured by electrochemistry.

An activation process was observed for MoB at pH ca. 0, and for Mo_2C at pH ca. 0 and 14. During this activation process, the activity of a freshly-prepared electrode gradually increased over the first several polarization measurements (Figure S3). Normally the catalytic current became stable after five scans. No activation process was observed for MoB at pH ca. 14. Figure 1 shows the 10th (and thus stable) polarization curves of MoB and Mo_2C-based electrodes at pH ca. 0 (1M H_2SO_4) and pH ca. 14 (1M KOH).
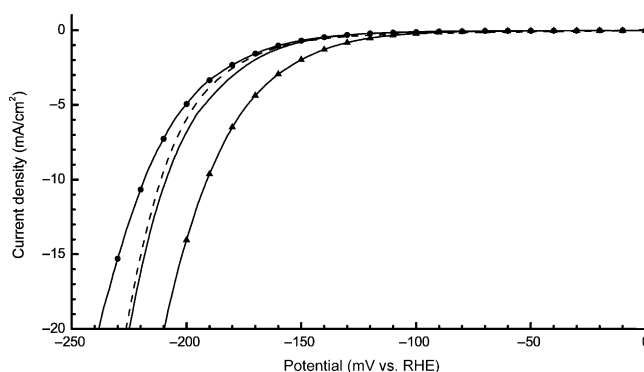

Figure 1. Polarization curves (10th) of MoB and Mo_2C at pH 0 and 14. Scan rate = 1 mV s^{-1}. MoB, pH 0, 2.5 mg cm^{-2} (-----); MoB, pH 14, 2.3 mg cm^{-2} (——●——); Mo_2C, pH 0, 1.4 mg cm^{-2} (——); Mo_2C, pH 14, 0.8 mg cm^{-2} (——▲——). The iR drop was corrected.

MoB and Mo_2C are active HER catalysts. The onsets of catalytic currents are observed at $\eta \cong 100$ mV. The overpotentials for a current density of 20 mA cm^{-2} are between 210 and 240 mV. The activities of MoB and Mo_2C are similar. At pH 0, their activity is also similar to previously reported amorphous MoS_x films and particles.[6] More importantly, MoB and Mo_2C catalyze HER at pH 14, where MoS_x is unstable. Surprisingly, the activity of MoB and Mo_2C at pH 14 is comparable to their activity at pH 0. In general, very few catalysts are active at both pH 0 and 14. Pt is one such catalyst.[11] Figure 2 shows that at the same current density, MoB and Mo_2C require about 100 mV more overpotential than Pt;[12] however, this decreased activity of MoB and Mo_2C

[*] H. Vrubel, Prof. Dr. X. Hu
Laboratory of Inorganic Synthesis and Catalysis
Institute of Chemical Sciences and Engineering
Ecole Polytechnique Fédérale de Lausanne (EPFL)
ISIC-LSCI, BCH 3305, Lausanne 1015 (Switzerland)
E-mail: xile.hu@epfl.ch
Homepage: http://lsci.epfl.ch

Supporting information for this article is available on the WWW under http://dx.doi.org/10.1002/anie.201207111.
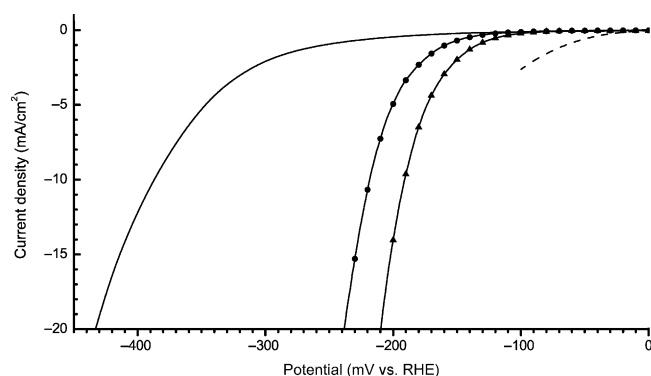
Figure 2. Polarization curves of MoB (——●——), Mo₂C (——▲——), Pt (-----), and Ni (——) at pH 14. The 10th consecutive curves for MoB, Mo₂C, and Ni, and the 1st curve for Pt after anodic activation are displayed. Scan rate = 1 mVs⁻¹. The iR drop was corrected.

might be compensated for by their higher abundance and lower cost. Ni is often used as the electrode for HER in basic solutions.[13] Figure 2 shows that the activity of MoB and Mo₂C is significantly higher than Ni. There is now interest in conducting HERs in neutral water,[7,14] so the activity of MoB and Mo₂C was also studied in pH 7 phosphate buffer. The onsets of catalytic waves are observed at about 100 mV, which is similar to those in acidic or basic solutions (Figure S5); however, the current densities at pH 7 are lower, probably because the transport of hydroxide ions is not as efficient under these conditions.

Tafel analysis was conducted on the polarization curves of MoB and Mo₂C catalysts (Figure S6). Tafel slopes of 54–59 mV/decade were found in the region of $\eta = $ ca. 100–220 mV (Table 1). The Tafel slopes are similar for both

Table 1: Results of Tafel analysis.

Entry	Cat.	pH	Tafel slope [mV/decade]	Exchange current density [mAcm⁻²]	Tafel region [mV]
1	MoB	0	55	1.4×10^{-3}	140–210
2	Mo₂C	0	56	1.3×10^{-3}	100–220
3	MoB	14	59	2.0×10^{-3}	140–230
4	Mo₂C	14	54	3.8×10^{-3}	100–220

catalysts at both pH values. The apparent exchange current densities are in the range of 10^{-3} mAcm⁻². The exchange current densities at pH 14 are slightly higher than at pH 0. This result indicates that MoB and Mo₂C catalysts are equally effective for water reduction (pH 14) and proton reduction (pH 0). Although Tafel analysis is commonly used to probe the mechanism of hydrogen evolution, it is difficult to apply such analysis in the current system, because the measured Tafel slopes are different from the limiting slopes of 29, 38, or 116 mV/decade.[15] However, slopes of 54–59 mV/decade rule out the possibility that the discharge reaction (Volmer step) is the rate-determining step, which would result in a Tafel slope of 116 mV/decade. We suspect that the Volmer step is rapid at each reaction center. However, as the MoB and Mo₂C

particles have a large size (μm) and irregular shape (Figure S2), the transport of electrons and/or protons might be hampered in certain regions, which gives rise to an overall Tafel slope that is larger than 29 or 38 mV/decade.

The hydrogen production efficiency of the MoB and Mo₂C catalysts were probed first by Galvanostatic electrolysis. A cathodic current density of 20.4 mAcm⁻² was chosen, which approaches the upper limit for a photoelectrochemical water splitting device (solar-to-hydrogen efficiency ca. 25%).[16] As shown in Figure S7, the potentials remained relatively stable over one hour. The amount of hydrogen produced during Galvanostatic electrolysis was measured, and the Faradaic efficiency for hydrogen evolution was calculated after correction of the activation process. At pH 14, no activation process is required for MoB, and Figure 3a shows that the Faradaic yield is 100% over
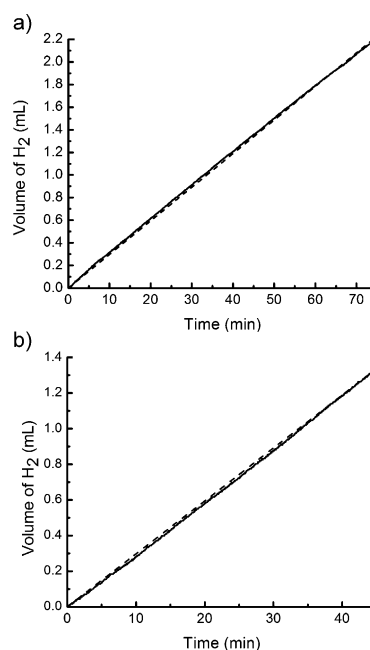

Figure 3. Current efficiency for HER under Galvanostatic electrolysis. a) MoB at pH 14; b) Mo₂C at pH 14 after an activation process of 30 min. The calculated H₂ lines (-----) represent the expected amount of H₂, assuming a quantitative Faradaic yield for H₂ formation. The measured H₂ lines (——) represent the experimentally detected H₂.

a period of 75 min. On the other hand, Mo₂C requires an activation process of about 30 min, which causes the Faradaic yield to be lower than 100% during this time (Figure S8). Once activated, however, the Faradaic yield becomes 100% within 45 min (Figure 3b). Analogous behaviors were observed at pH 0. After activation, both MoB and Mo₂C have a 100% Faradaic yield for hydrogen evolution (Figure S8). Thus, after activation, the hydrogen production efficiency for all catalysts is quantitative.

The hydrogen production efficiency of the MoB and Mo₂C catalysts was also probed by potentiostatic electrolysis after activation. At pH 0 and $\eta = 250$ mV, Mo₂C and MoB had current densities of 19 and 17 mAcm⁻², respectively (without iR drop correction). Figure S9 shows that the Faradaic yields

(and thus the hydrogen production efficiency) are quantitative. At pH 14 and $\eta = 250$ mV, Mo_2C and MoB had current densities of 6 and 5 mA cm^{-2}, respectively. The lower current densities compared to those at pH 0 are probably due to a higher solution resistance.[17] Figure S10 shows that the Faradaic yields and the hydrogen production efficiency are again quantitative.

To probe the nature of the activation process, MoB and Mo_2C before and after activation were analyzed by X-ray photoelectron spectroscopy (XPS). The analysis of carbon was complicated by the presence of graphite and adventitious impurities in the carbon-paste electrodes. The analysis of Mo, however, revealed important information. In accordance with earlier studies, the surfaces of MoB and Mo_2C particles were contaminated with molybdenum oxides,[18] such as MoO_3 and MoO_2, before activation (Figure 4). After activation by
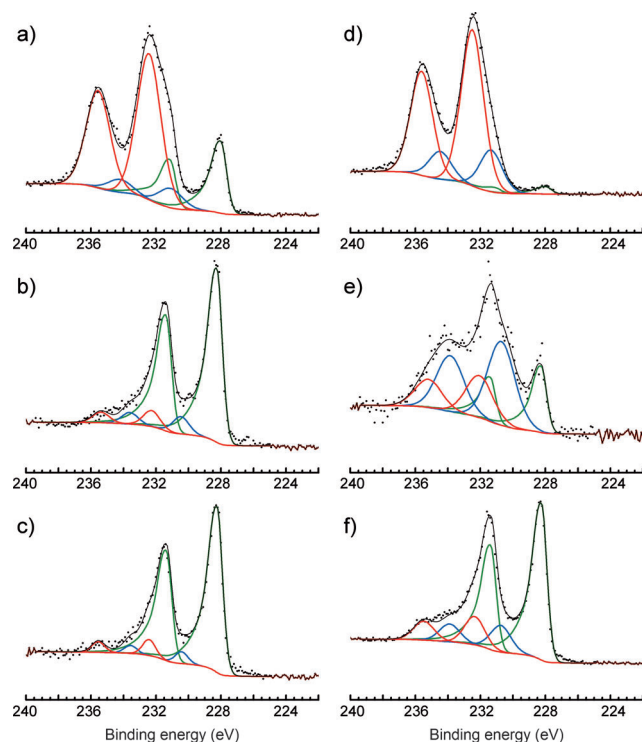
Figure 4. XPS Mo spectra of Mo_2C and MoB before and after activation. a) Mo_2C sample before activation. b) Mo_2C sample after activation at pH 0. c) Mo_2C sample after activation at pH 14. d) MoB sample before activation. e) MoB sample after activation at pH 0. f) MoB sample after activation at pH 14. Experimental data (•••••), fitting envelope (——), Mo_2C (a–c; ——), MoB (d–f; ——), MoO_2 (——), MoO_3 (——).

Galvanostatic electrolysis for 15 min at 10 mA cm^{-2}, the amounts of MoO_3 and MoO_2 greatly diminished, and the major Mo-containing species are MoB and Mo_2C for the respective samples (Figure 4).[19] Figure S11 shows that MoO_2, MoO_3, and Mo metal are not efficient catalysts for HER. Thus, we propose that the activation process was related to the reductive removal of surface oxides. For MoB in base, the activation process was fast because of the dissolution of the materials (see below); therefore this process was not visible.

The long-term stability of the MoB and Mo_2C catalysts was examined by extended electrolysis at fixed potentials. Figure 5 shows that at pH 0, the catalytic currents remained ca. 10 mA cm^{-2} at $\eta = $ ca. 200 mV for both MoB and Mo_2C
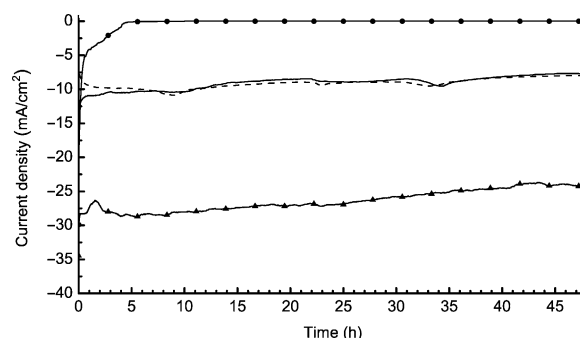
Figure 5. Time dependence of catalytic currents during electrolysis over 48 h for MoB and Mo_2C at pH 0 and 14. The iR drop was corrected. MoB, pH 0, -195 mV (-----); MoB, pH 14, -200 mV (——•——); Mo_2C, pH 0, -195 mV (——); Mo_2C, pH 14, -160 mV (——▲——).

modified carbon-paste electrodes during 48 h. These catalysts thus appear stable in acidic conditions. Because the paraffin binder for the carbon-paste electrodes could be gradually dissolved in basic solutions, the MoB and Mo_2C modified carbon-paste electrodes were not suitable for long-term stability studies in basic solution. For such a study, MoB and Mo_2C disk electrodes were fabricated by pressing mixtures of catalyst powders and Teflon. Figure 5 shows that the catalytic current from the Mo_2C disk electrode was stable during 48 h at pH 14 as well. On the other hand, the MoB disk electrode was unstable, and the catalytic current decayed after one hour. Visual inspection indicated that the MoB disk electrode was corroded.

In conclusion, MoB and Mo_2C particles have been shown to be excellent catalysts for hydrogen evolution. The catalysts are made of non-precious elements and operate in both acidic and basic solutions. The catalysts are stable during electrolysis (except for MoB at pH 14) and the current efficiency is quantitative. The activity in alkaline solutions is surprisingly high and is comparable to that in acidic solutions. Furthermore, there is tremendous potential for improvement with these catalysts. Although the catalytic activity of large and irregular particles is already high, we expect better activity from more defined nanoparticles, which will be a target of follow-up studies. The large particles are insoluble and not solution processable. This obliged us to press the particles onto a soft carbon-paste electrode to measure their catalyst activity. As a result, the loading of the catalyst was relatively high. If the same materials can be produced in a soluble colloidal form, they may be cast as thin films using spray-casting or spin-coating techniques; the catalytic performance with respect to catalyst loading would then be expected to dramatically increase. Last but not least, the catalytic properties of these molybdenum compounds raise an interesting mechanistic question: how is hydrogen produced? Does Mo behave like other metals such as Pt, Ni, and Hg, or are

bridging hydride species such as Mo-H-B and Mo-H-C involved? Further spectroscopic, electrochemical, and computational studies are warranted.[20]

[1] N. S. Lewis, D. G. Nocera, *Proc. Natl. Acad. Sci. USA* **2006**, *103*, 15729–15735.

[2] a) T. R. Cook, D. K. Dogutan, S. Y. Reece, Y. Surendranath, T. S. Teets, D. G. Nocera, *Chem. Rev.* **2010**, *110*, 6474–6502; b) M. G. Walter, E. L. Warren, J. R. McKone, S. W. Boettcher, Q. X. Mi, E. A. Santori, N. S. Lewis, *Chem. Rev.* **2010**, *110*, 6446–6473.

[3] a) V. Artero, M. Fontecave, *Coord. Chem. Rev.* **2005**, *249*, 1518–1535; b) M. Rakowski DuBois, D. L. DuBois, *Chem. Soc. Rev.* **2009**, *38*, 62–72; c) P. W. Du, R. Eisenberg, *Energy Environ. Sci.* **2012**, *5*, 6012–6021; d) M. Wang, L. Chen, L. C. Sun, *Energy Environ. Sci.* **2012**, *5*, 6763–6778.

[4] a) B. Hinnemann, P. G. Moses, J. Bonde, K. P. Jorgensen, J. H. Nielsen, S. Horch, I. Chorkendorff, J. K. Norskov, *J. Am. Chem. Soc.* **2005**, *127*, 5308–5309; b) T. F. Jaramillo, K. P. Jorgensen, J. Bonde, J. H. Nielsen, S. Horch, I. Chorkendorff, *Science* **2007**, *317*, 100–102; c) J. Bonde, P. G. Moses, T. F. Jaramillo, J. K. Norskov, I. Chorkendorff, *Faraday Discuss.* **2009**, *140*, 219–231.

[5] a) T. F. Jaramillo, J. Bonde, J. D. Zhang, B. L. Ooi, K. Andersson, J. Ulstrup, I. Chorkendorff, *J. Phys. Chem. C* **2008**, *112*, 17492–17498; b) A. B. Laursen, S. Kegnaes, S. Dahl, I. Chorkendorff, *Energy Environ. Sci.* **2012**, *5*, 5577–5591; c) Y. D. Hou, B. L. Abrams, P. C. K. Vesborg, M. E. Bjorketun, K. Herbst, L. Bech, A. M. Setti, C. D. Damsgaard, T. Pedersen, O. Hansen, J. Rossmeisl, S. Dahl, J. K. Norskov, I. Chorkendorff, *Nat. Mater.* **2011**, *10*, 434–438; d) D. Merki, X. L. Hu, *Energy Environ. Sci.* **2011**, *4*, 3878–3888; e) H. I. Karunadasa, E. Montalvo, Y. J. Sun, M. Majda, J. R. Long, C. J. Chang, *Science* **2012**, *335*, 698–702; f) Y. G. Li, H. L. Wang, L. M. Xie, Y. Y. Liang, G. S. Hong, H. J. Dai, *J. Am. Chem. Soc.* **2011**, *133*, 7296–7299; g) Z. B. Chen, D.

[6] a) D. Merki, S. Fierro, H. Vrubel, X. L. Hu, *Chem. Sci.* **2011**, *2*, 1262–1267; b) H. Vrubel, D. Merki, X. L. Hu, *Energy Environ. Sci.* **2012**, *5*, 6136–6144.

[7] H. I. Karunadasa, C. J. Chang, J. R. Long, *Nature* **2010**, *464*, 1329–1333.

[8] D. V. Esposito, S. T. Hunt, Y. C. Kimmel, J. G. G. Chen, *J. Am. Chem. Soc.* **2012**, *134*, 3025–3033.

[9] M. C. Weidman, D. V. Esposito, Y. C. Hsu, J. G. Chen, *J. Power Sources* **2012**, *202*, 11–17.

[10] J. C. Peters, A. L. Odom, C. C. Cummins, *Chem. Commun.* **1997**, 1995–1996.

[11] R. Subbaraman, D. Tripkovic, D. Strmcnik, K. C. Chang, M. Uchimura, A. P. Paulikas, V. Stamenkovic, N. M. Markovic, *Science* **2011**, *334*, 1256–1260.

[12] The *i–V* curve is shown up to $V = -100$ mV for Pt because mass-transport becomes rate-limiting at more negative potentials (Supporting Information, Figure S4).

[13] G. Schiller, R. Henne, P. Mohr, V. Peinecke, *Int. J. Hydrogen Energy* **1998**, *23*, 761–765.

[14] S. Y. Reece, J. A. Hamel, K. Sung, T. D. Jarvi, A. J. Esswein, J. J. H. Pijpers, D. G. Nocera, *Science* **2011**, *334*, 645–648.

[15] J. O. M. Bockris, E. C. Potter, *J. Electrochem. Soc.* **1952**, *99*, 169–186.

[16] Z. B. Chen, T. F. Jaramillo, T. G. Deutsch, A. Kleiman-Shwarsctein, A. J. Forman, N. Gaillard, R. Garland, K. Takanabe, C. Heske, M. Sunkara, E. W. McFarland, K. Domen, E. L. Miller, J. A. Turner, H. N. Dinh, *J. Mater. Res.* **2010**, *25*, 3–16.

[17] The resistance is about 1.7 Ohm at pH 0, and 4 Ohm at pH 14.

[18] a) B. Brox, I. Olefjord, *Surf. Interface Anal.* **1988**, *13*, 3–6; b) J. L. G. Fierro, E. Salazar, J. A. Legarreta, *Surf. Interface Anal.* **1985**, *7*, 97–104; c) K. Oshikawa, M. Nagai, S. Omi, *J. Phys. Chem. B* **2001**, *105*, 9124–9131.

[19] E. C. Weigert, D. V. Esposito, J. G. G. Chen, *J. Power Sources* **2009**, *193*, 501–506.

[20] J. Greeley, T. F. Jaramillo, J. Bonde, I. B. Chorkendorff, J. K. Norskov, *Nat. Mater.* **2006**, *5*, 909–913.